Ref. Ares(2020)1277510 - 28/02/2020

HORIZON 2020

Research Infrastructures

H2020-INFRAIA-2014-2015

INFRAIA-1-2014-2015 Integrating and opening existing national and regional research infrastructures of European interest

ENSAR2

European Nuclear Science and Application Research 2

Grant Agreement Number: 654002

D10.6 Final Report on R&D on segmented p-type coaxial detectors

Version: 6.0
Author: A. Gadea, D. R. Napoli, D. de Salvador
Date: 28/02/2020

PROJECT AND DELIVERABLE INFORMATION SHEET

ENSAR2 Project Ref. №	654002
Project Title	European Nuclear Science and Application Research 2
Project Web Site	http://www.ensarfp7.eu/
Deliverable ID	D10.6
Deliverable Nature	Final Report
Deliverable Level*	PU
Contractual Date of Delivery	February 29th 2020
Actual Date of Delivery	February 29th 2020
EC Project Officer	René Martins

* The dissemination levels are indicated as follows: PU – Public, PP – Restricted to other participants (including the Commission Services), RE – Restricted to a group specified by the consortium (including the Commission Services). CO – Confidential, only for members of the consortium (including the Commission Services).

DOCUMENT CONTROL SHEET

Document	Title: Final Report on R&D on segmented p-type coaxial detectors	
	ID: D10.6	
	Version: 6.0	
	Available at: http://www.ensarfp7.eu/	
	Software Tool: Microsoft Office Word 2007	
	File:	
Authorship	Written by:	A. Gadea, D.R. Napoli, D. de Salvador
	Contributors:	S. Bertoldo, V. Boldrini, C. Carraro, S. Cartu-ran, G. Maggioni, R. Milazzo, E. Napolitani, W. Raniero, S. Riccetto, F. Sgarbossa
	Reviewed by:	D. Ackermann, GANIL
	Approved by:	M.N. Harakeh, KVI Cart

DOCUMENT STATUS SHEET

Version	Date	Status	Comments
4.0	26/02/2020	For internal review	
5.0	27/02/2020	For internal review	
6.0	29/02/2020	Submitted on EC Participant Portal	
		Final version	

DOCUMENT KEYWORDS

Keywords	Position-sensitive germanium detectors, Gamma-imaging techniques, Hyper-pure germanium detector associated techniques

Disclaimer

This deliverable has been prepared by Work Package 10 (PSeGe - Position-Sensitive Germanium Detectors) of the Project in accordance with the Consortium Agreement and the Grant Agreement n°654002. It solely reflects the opinion of the parties to such agreements on a collective basis in the context of the Project and to the extent foreseen in such agreements.

Copyright notices

© 2016 ENSAR2 Consortium Partners. All rights reserved. This document is a project document of the ENSAR2 project. All contents are reserved by default and may not be disclosed to third parties without the written consent of the ENSAR2 partners, except as mandated by the European Commission contract 654002 for reviewing and dissemination purposes.
All trademarks and other rights on third party products mentioned in this document are acknowledged as own by the respective holders.

TABLE OF CONTENTS

LIST OF FIGURES

REFERENCES AND APPLICABLE DOCUMENTS

[1] H.L. Malm, IEEE Trans. Nucl. Sci. 22, 140 (1975).
[2] J. Eberth, J. Simpson, Prog. Part. Nucl. Phys. 60, 283 (2008).
[3] G.S. King III, F.T. Avignone III, C.E. Cox, T.W. Hossbach, W. Jennings, J.H. Reeves, Nucl. Instrum. Methods Phys. Res. A 595, 599 (2008).

[4] G.S. Hubbard, E.E. Hailer, W.L. Hansen, IEEE Trans. Nucl. Sci. 24, 161 (1977).
[5] E. Bruno, G.G. Scapellato, G. Bisognin, E. Carria, L. Romano, A. Carnera, F. Priolo, J. Appl. Phys. 108, 124902 (2010).
[6] W.L. Hansen, E.E. Haller, IEEE Trans. Nucl. Sci. 24, 61 (1977).
[7] P.N. Luke, C.P. Cork, N.W. Madden, C.S. Rossington, M.F. Wesela, IEEE Trans. Nucl. Sci. 39, 590 (1992).
[8] M. Amman, P.N. Luke, S.E. Boggs, Nucl. Instrum. Methods Phys. Res. A 579, 886 (2007).
[9] Q. Looker, Fabrication Process Development for High- Purity Germanium Radiation Detectors with Amorphous Semiconductor Contacts, PhD Thesis, University of California, Berkeley (2014).
[10] Q. Looker, M. Amman, K. Vetter, Nucl. Instrum. Methods Phys. Res. A 777, 138 (2015).
[11] E.L. Hull, R.H. Pehl, J.R. Lathrop, B.E. Suttle, Nucl. Instrum. Methods Phys. Res. A 626-627, 39 (2011).
[12] T. Nishimura, K. Kita, A. Toriumi, Appl. Phys. Lett. 91, 123123 (2007).
[13] E. Hull, https://science.energy.gov/~/media/np/pdf/ sbir%20sttr/SBIR STTR 2015/Day%202/Hull Thin Window Presentation 20150807 for NP website.pdf.
[14] Y. Bao, K. Sun, N. Dhar, M.C. Gupta, IEEE Photon. Technol. Lett. 26, 1422 (2014).
[15] J.M. Poate, J.W. Mayer, Laser Annealing of Semiconductors (Academic Press, New York, 1982).
[16] G. Mannino, V. Privitera, A. La Magna, E. Rimini, E. Napolitani, G. Fortunato, L. Mariucci, Appl. Phys. Lett. 86, 51909 (2005).
[17] R. Milazzo, E. Napolitani, G. Impellizzeri, G. Fisicaro, S. Boninelli, M. Cuscuna, D. De Salvador, M. Mastromatteo, M. Italia, A. La Magna, G. Fortunato, F. Priolo, V. Privitera, A. Carnera, J. Appl. Phys. 115, 53501 (2014).
[18] G. Impellizzeri, E. Napolitani, S. Boninelli, G. Fisicaro, M. Cuscuna`, R. Milazzo, A. La Magna, G. Fortunato, F. Priolo, V. Privitera, J. Appl. Phys. 113, 113505 (2013).
[19] D.H. Lowndes, T.W. Raudorf, Nucl. Instrum. Methods Phys. Res. A 240, 362 (1985).
[20] Umicore datasheet of product number 95097, Lot number 12207.
[21] G. Maggioni, F. Sgarbossa, E. Napolitani, W. Raniero, V. Boldrini, S.M. Carturan, D.R. Napoli, D. De Salvador, Mater. Sci. Semicond. Process. 75, 118 (2018).
[22] G. Maggioni, D.R. Napoli, J. Eberth, M. Gelain, S. Carturan, M.G. Grimaldi, S. Tat`ı, Eur. Phys. J. A 51, 141 (2015).
[23] G.F. Knoll, Radiation Detection and Measurement, 2nd edition (J. Wiley & Sons, Inc., New York, 1989).
[24] V. Boldrini et al., Characterization of thermally-induced doping defects in bulk HPGe, in preparation.
[25] R. Milazzo, G. Impellizzeri, D. Piccinotti, D. De Salvador, A. Portavoce, A. La Magna, G. Fortunato, D. Mangelinck, V. Privitera, A. Carnera, E. Napolitani, Appl. Phys. Lett. 110, 11905 (2017).
[26] V. Boldrini, S. Carturan, G. Maggioni, E. Napolitani, D.R. Napoli, R. Camattari, D. De Salvador, Appl. Surf. Sci. 392, 1173 (2017).
[27] S. Prucnal, L. Rebhole, W. Skorupa, Mater. Sci. Semicond. Process. 62, 115 (2017).

LIST OF ACRONYMS AND ABBREVIATIONS

HPGe	Hyper-Pure Germanium, i.e. Ge with an extremely low net impurity concentration (around 10^{10} atoms cm^{-3})
AGATA	Advanced Gamma-Tracking Array, first gamma-tracking array, constructed in collaboration by nearly 50 European institutes involved in nuclear structure research studies.
GRETA	Similar array to AGATA but constructed in United States of America
SEM	Secondary Electron Microscope
SIMS	Secondary Ion Mass Spectrometry
RBS	Rutherford backscattering spectrometry

EXECUTIVE SUMMARY

Presently n-type Ge detectors are the only ones that can be used as position-sensitive Ge detectors in tracking detector arrays for in-beam gamma spectroscopy, since position sensitivity is achieved by segmenting the outer contact. The possibility to produce p-type position-sensitive detectors for in-beam spectroscopy should improve the functional performance of the detectors, over long experimental campaigns, due to the slower degradation of the electron signal, by neutron-damage, as well as the higher recovering capability after annealing.
The most promising candidates for n-contact dopants have been evaluated and tested, antimony (Sb) has proven to match the requirements and to be compatible with the required purity and production conditions.
New technology for production of segmented contacts, in Ge detectors, based on Laser Thermal Annealing has been tested. Fully functional, small dimension prototypes, of segmented n-contacts in p-type HPGE crystals have been produced.

INTRODUCTION

High purity germanium (HPGe) detectors are diodes obtained starting from Ge single crystals with an extremely low net impurity concentration (around 10^{10} atoms cm^{-3}). The electron-barrier and hole-barrier contacts of the diode are placed on the opposite sides of the Ge crystal in order to achieve the full charge depletion of the intrinsic volume, without giving rise to sizable leakage currents. For this last reason, the surface of the intrinsic Ge between the two contacts needs to be passivated. Several technologies have been developed for the fabrication of electron-barrier contacts such as vacuum-deposited metal layers, which produce Schottky barriers at the metal/Ge interface [1]. In commercial detectors, boron implantation is commonly used for producing a thin (< 300nm) electron-barrier contact, which can be segmented in a variety of geometries. It provides thin dead layers for gamma detection. This last feature, which assures a very limited decrease of the active volume of the detector, is particularly important for complex HPGe detectors (such as highly segmented detectors used, e.g., for new spectrometers like AGATA or GRETA), wherein each point of the HPGe crystal concurs to the reconstruction of the gamma-ray tracks.

On the other hand, in the case of hole-barrier contacts, the present-day commercial standard is a thick (several hundreds of μm) contact obtained by diffusion of evaporated lithium using a standard annealing process at temperatures of 300–400 ◦C [2]. Though robust and reliable, the Li contact has several drawbacks: i) its thickness; ii) it is thermally unstable and the annealing cycles at T ≥ 100 °C, necessary to recover the radiation damage produced in high energy experiments, cause the lithium to diffuse further; iii) it can be only coarsely segmented by grinding or using wide intersegment gaps [3] and the electrical insulation between the segments can be easily jeopardised due to the low dopant stability. For these reasons, alternative methods for the production of thin and thermally stable hole-barrier contacts are very appealing and would enormously boost the improvement of HPGe detector technology. In the past, phosphorus ion implantation was implemented resulting in thin n+ contacts, but, unlike B implantation, the electrical activation of implanted P atoms requires an additional annealing step at relatively high temperatures (350–400 ◦C) [4]. This step can easily induce contaminant diffusion and then harm the charge collection features of the germanium detector. Implantation of higher mass elements like, for example, Sb has caused the production of unwanted, severe damage in the crystal structure and their use has been banned [5].

In the last years, amorphous-germanium and amorphous-silicon contacts have been increasingly attracting the interest of the community owing to their low fabrication complexity, low thickness, easy segmentation and the capability of sustaining reasonably high electric fields [6– 8]. Unfortunately, the stability and reproducibility of these contacts is not high enough and the leakage currents are higher as compared to a standard Li contact [9–11]. Recently, a new Y-based contact has been proposed: an yttrium film is sputtered on the HPGe crystal and gives rise

to a hole-barrier contact at the interface Y/Ge [11]. This contact is thin and can be, in principle, segmented using photolithography, but its barrier properties are not fully understood, since the barrier height is reported to be quite low (0.13 eV [12]), and can be strongly dependent on the features of the Y/Ge interface. Hole-barrier contacts based on Ag have also been very recently proposed [13], but the characterisation of their properties is still ongoing.

Among the different techniques implemented for making contacts in semiconductor materials, laser annealing appears to be very appealing for HPGe applications. This technique, which exploits laser pulses with high energy density to induce the melting of a very thin surface layer followed by ultra-fast liquid phase epitaxial regrowth, has been widely investigated in Si and Ge for microelectronics applications [14–18], because it allows to produce highly doped contacts, nearly ideal p-n junctions and recrystallized near-surface regions, which are free of extended defects. In spite of the fact that all the remaining Ge bulk (> 10 μm depth) remains at a temperature that is very close to room temperature during the laser treatment, thus preventing the thermally-induced diffusion of contaminants inside the crystal, this technique has been seldom considered for the production of HPGe devices. Lowndes and Raudorf [19] used it for high energy charged particle detectors, carrying out pulsed laser diffusion of phosphorus from a liquid source into p-type HPGe, resulting in the formation of a thin (< 1 μm) hole-barrier contact and an n+-p junction. In that case, maybe due to limited performance of the used laser (a ruby laser), the onset of a laser damage at energy densities greater than 1 J cm^{-2} was pointed out by the increasingly dull appearance of the Ge surface.

SECTION 1 NEW CONTACTS FOR P-TYPE CRYSTALS

In this work, we have obtained for the first time a working thin hole-barrier contact in HPGe by using an innovative technique based on the sputter deposition of an antimony film on germanium surface, followed by a pulsed laser annealing, which causes Sb diffusion into Ge. The extremely high purity of Sb sputter targets, which can be found nowadays on the market, makes them compliant with the severe requirements of the production process of HPGe detectors.

First, a small prototype of a planar detector was produced with this new Sb-based contact on the one side and with a standard boron implanted contact on the other side. The detector properties were investigated using different gamma-ray sources. In order to evaluate correctly the properties of this prototype, it has to be pointed out that the choice of the geometrical configuration of the contacts was made to facilitate the pulsed laser treatment at the expense of the detector performance.

The initial crystal was a (100) p-type, 2 mm thick HPGe ($(0.93 \pm 0.03) \times 10^{10}$ atoms cm^{-3} impurity concentration) wafer (Umicore [20]) with as-cut surfaces was used for the experiments. Both wafer sides were manually polished to smooth the surface. The wafer was then cut by a dicer into 10×10 mm^2 samples and subsequently cleaned with hot 2-propanol, hot deionised (DI) water and HF 10% to remove the dicing adhesive residue and native oxides. The square HPGe substrates were chemically etched in 3:1 HNO_3 65%: HF 40% solution (all acids were of reagent grade, Carlo Erba Reagents srl) for at least 5 minutes in order to remove the mechanically damaged surface layer. Chemical etching gave rise to a decrease of the substrate thickness 1.9 mm. After this step, the square samples underwent different treatments depending on their final use:

i) samples for Secondary Electron Microscope (SEM) and Secondary Ion Mass Spectrometry (SIMS) characterisations were directly put in the sputtering deposition equipment for Sb deposition;

ii) samples to be used as detectors (detector samples) underwent boron implantation (23 keV, 1×10^{15} at cm^{-2}) on one side in order to make the electron-barrier contact, before proceeding with the Sb film deposition, which was carried out in a central circular region (5 mm diameter) on the other side of the sample, after masking the remaining surface by kapton tape.

The Sb sputtering equipment consisted of a stainless-steel vacuum chamber evacuated by a turbomolecular pump at a base pressure lower than 1×10^{-4} Pa. The glow discharge-sustaining device was a 5.08 cm cylindrical magnetron-sputtering source connected to a radio frequency power generator (600 W, 13.56 MHz) through a matching box. The deposition parameters used for all the films were: direct RF power 30 W; target-to-substrate distance 14 cm; working gas Ar (99.9999% purity); Ar flow 3.33×10^{-7} $m^3 s^{-1}$. A mass flow controller regulated the working gas flow and the chamber was continuously pumped during the deposition in order to reduce atmospheric contamination by wall outgassing. Pure Sb (99.999%, ACI Alloys) with a very low Cu content (≤ 0.01 mg/kg) was used as a target. The Sb deposition rate, as determined by Rutherford backscattering spectrometry (RBS), was 13.3 nm min^{-1} (*i.e.* 3.76×10^{16} atoms cm^{-2} min^{-1} with a Sb density of 3.27×10^{22} atoms cm^{-3}) [21]. The duration of the deposition run was fixed in order to achieve a film thickness of 2nm.

A pulsed Nd:YAG solid-state laser, characterised by 7 ns pulse duration and 10 Hz repetition rate, was used for the Sb diffusion. The laser light was in the UV range (355 nm) and the energy density deposited on the sample during the annealing treatment (which consisted in 1 pulse) was 400mJ cm^{-2}.

After laser annealing, the intrinsic surface of the detector sample was passivated by etching in the 3:1 HNO_3 65%: HF 40% acid solution for 20 s and then quenching it directly in methanol (Erbatron, Carlo Erba) [22]. The detector sample was then blown on with dry nitrogen. During etching, both contacts were protected by kapton tape.

The surface morphology of the samples was investigated by SEM (Tescan Vega3 XM). SIMS profiles were done on laser-annealed samples, by using a Cameca IMS-4f instrument with an O_2^+ beam, to characterise the Sb diffusion profiles.

For all the measurements, the detector sample was mounted on a commercial standard cryostat where the crystal mounting has been modified *ad hoc* for these tests (Fig. 1) and cooled to (91 ± 1) K. A 1.0mm thick indium foil was inserted between each side of the detector and the metal supports, in order to improve the electrical contact. The same cryostat was used for the determination of the detector properties. Standard calibrated gamma-ray sources of ^{241}Am, ^{152}Eu and ^{133}Ba, provided by the supplier with a calibration certificate, which attests that the activity of the source was determined by comparison with a reference source of the same construction, were used for the detector tests. The sources were placed as close as possible to the lateral side of the detector in order to minimise the absorbing material thickness between source and detector, *i.e.* 1 mm Al for the mounting cap and 1 mm Al for the external end cap (Fig. 1). Detector properties were measured by using the ^{241}Am source, while the other two sources were used for the energy calibration. Analog NIM electronics was used for the detector measurements: an ORTEC preamplifier (model 137), an ORTEC spectroscopy amplifier (model 672) with 6μs shaping time, a CAEN HV power supply (model N1471A, ±5.5kV, 300μA max output, 5nA resolution) and an ORTEC Easy-MCA 8K with Maestro software.

The surface morphology after laser doping was examined using SEM analysis and the results are shown in Fig. 2. At this laser energy density (400mJ cm^{-2}), the surface remains as smooth as before treatment (Figs. 2a and 2b). This is particularly impressive if it is compared to the surface of Sb-coated Ge annealed with a standard treatment (fast annealing, see Fig. 2c and also SEM images in ref. [21]): in the latter case, at temperatures well below the Ge melting point ($T \geq 570^{\circ}$C), a plethora of defects, consisting in micro-grains and holes, appeared on the whole surface. The lack of any visible defects in the laser-annealed samples is probably due to the complete regrowth of the original Ge crystal structure following the surface melting. The SIMS Sb diffusion profile in the first 200 nm of thickness in a laser-annealed Ge sample is shown in Fig. 2d: as can be observed, the Sb concentration is higher than 1×10^{21} atoms cm^{-3} in the first 30nm, with a maximum of 2×10^{21} atoms cm^{-3} at the surface, and then rapidly decreases down to 1×10^{18} atoms cm^{-3} within the first 100nm of depth. As compared to the fast-annealed samples [21], the average concentration is significantly higher (almost three orders of magnitude) and the diffusion depth is lower (less than

100nm instead of almost 200nm). These data show that the laser annealing process gives rise to a very thin contact, especially as compared to the very thick Li contact used in commercial HPGe detectors, and avoids any damage to the crystal structure.

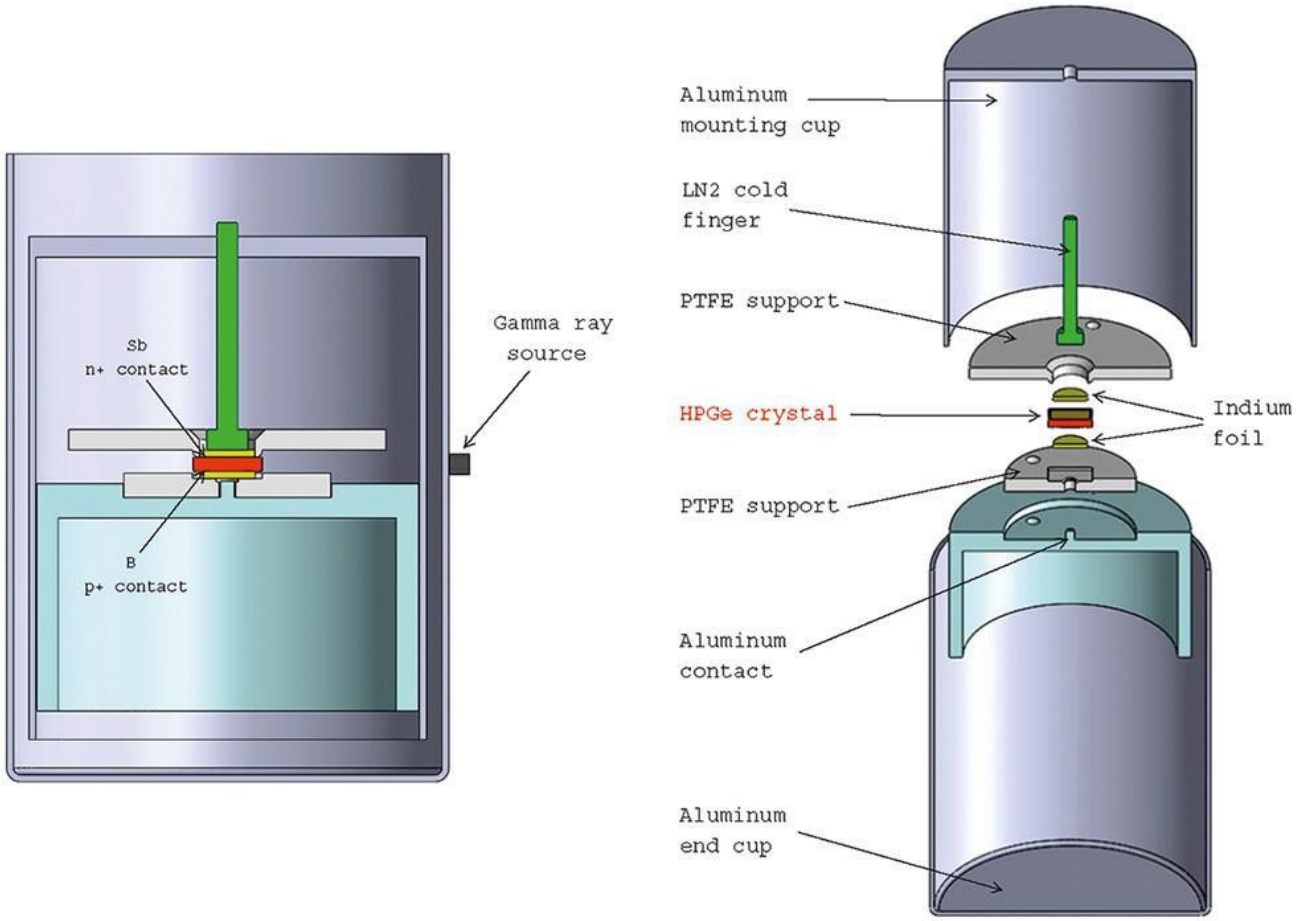

Figure 1. Layout scheme of the cryostat and supports of the HPGe crystal. The calibrated gamma-ray source is put on the side of the detector.

Fig. 3 shows the results of the measurement of the reverse leakage current of the cooled detector sample obtained by- passing the preamplifier stage (diode-test configuration) in the same cryostat described above. The reverse bias current is very low (below 5pA) until 10V, then it increases but still keeping low values (less than 30pA) up to 20V and afterwards it continues to increase at higher bias voltages (not shown in the figure), reaching 2nA at 40V. It is noteworthy that these very low values of current were obtained without using a guard ring, thus showing the effectiveness of the passivation procedure of the lateral intrinsic surface of the detector. In Fig. 3, the direct current measured at 1V is also shown (red dot): its significantly higher value (more than 10μA) compared to the reverse current at the same voltage highlights the diode behaviour of this detector, which is due to the successful formation of the n^+-p junction close to the Sb-doped contact. In order to evaluate the performance of the Sb-doped layer as a hole-barrier contact, the reverse leakage current under operating conditions of the detector has to be analysed, *i.e.* at bias voltages close to the depletion voltage ($\underline{V_d}$). The depletion voltage $\underline{V_d}$ is usually defined as the reverse bias voltage required to extend the depletion region through the full thickness of the detector, thus creating a totally depleted detector [23]. If surface effects can be neglected, $\underline{V_d}$ is given by the following equation [23]:

$$\underline{V_d} = eN\,d^2/2\varepsilon'$$

where e is the electronic charge, N is the impurity concentration in the bulk, d the detector thickness and ε the dielectric constant of germanium. In the case of the present detector, the impurity concentration was not measured after the laser treatment, but a value close to the pristine HPGe ($(0.93 \pm 0.03) \times 10^{10}$ atoms cm^{-3}, as given by Umicore) is expected, taking into account that the measurement of a sample treated with 4 laser pulses instead of 1, did not show any contamination [24]. With this value and assuming that the thickness of both n^+ and p^+ contacts is negligible with respect to the detector thickness, $\underline{V_d}$ would be found to be around 25V. However, taking into account the particular geometrical conformation of the Sb-doped contact, whose circular shape does not allow to achieve a uniform electrical field in the whole crystal volume, particularly near the corners, a slightly higher depletion voltage is expected. Nevertheless, as can be seen in Fig. 3, the low leakage current even at voltages as high as 40V shows that the hole barrier produced by the Sb-doped layer is very effective even at the full detector depletion.

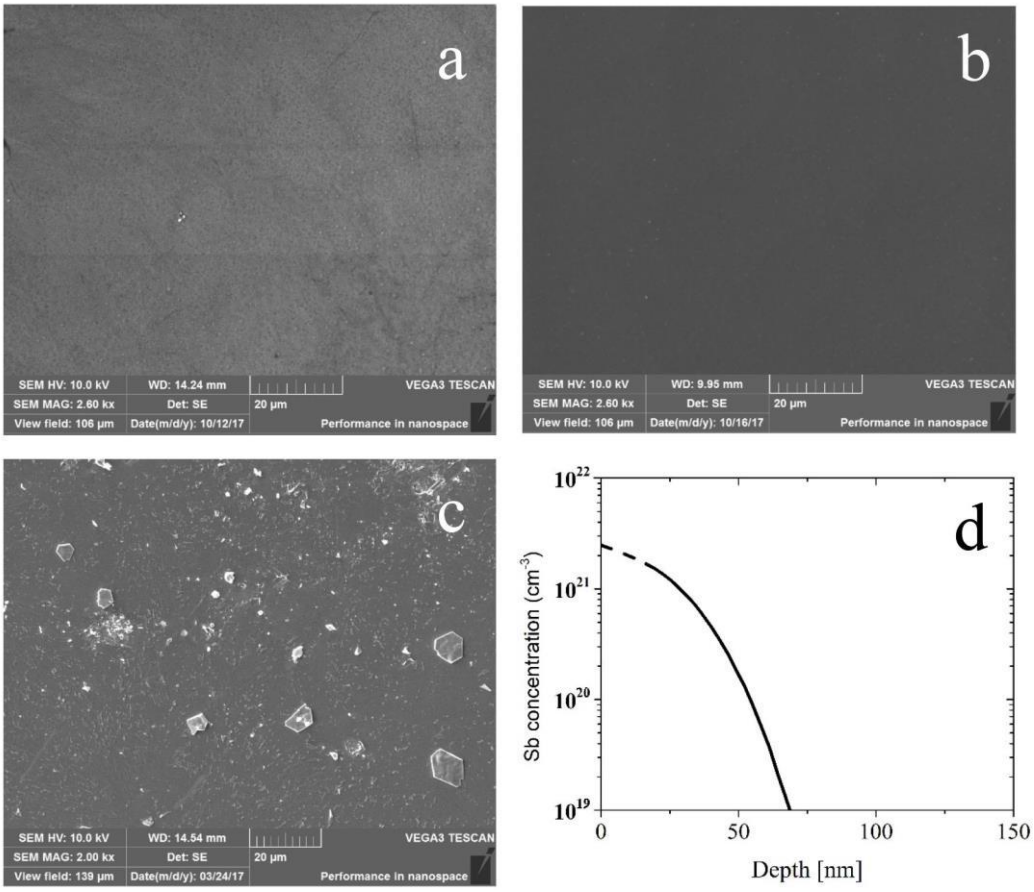

Figure 2. SEM images of the antimony-doped germanium surface: a) before laser annealing; b) after laser annealing; c) after fast annealing at 574°C for 30 minutes (see ref. [21] for experimental details); d) SIMS chemical concentration profile of antimony diffused in germanium after laser annealing.

The spectroscopic properties of the detector were investigated using three calibrated gamma-ray sources. Fig. 4 shows the ^{241}Am photopeak (E = 59.54keV) integral and energy resolution as a function of the applied bias voltage. The integral was calculated after background subtraction and normalisation to the acquisition live time. As can be seen, the integral is steadily increasing with the bias voltage: at 18 V the integral is three times the value at 2 V. This

increase is essentially due to the increase of the depleted volume in the detector. Also, the energy resolution shows a dependence on the applied voltage, ranging from 0.62 to 1.16keV (Fig. 4). At low bias voltages, when the detector volume is becoming more and more depleted, only a slight improvement of the resolution is observed at increasing voltage maybe due to the progressive decrease of the detector capacitance. This improvement continues until a bias of about 12V. It is worth considering that the 1% measured resolution is close to the best value, which can be obtained with this kind of detectors. A further increase of the bias voltage gives rise to an increase of the noise and to a drift of the baseline, which both make the energy resolution rapidly worse. This worsening is expected taking into account that, when the intensity of the electric field starts to become significant also in the regions close to the intrinsic surface and in the detector corners, the effects of the dead layers produced by the surface passivation on the charge collection become important as already shown in a previous work [22]. As a result, the increase in the photopeak integral occurring at the higher bias voltages is achieved to the detriment of the energy resolution.

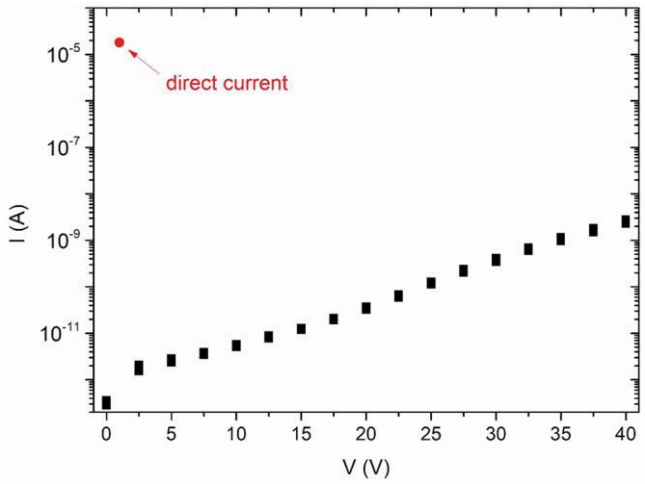

Figure 3. *I-V* curve of the Sb-doped detector measured in the diode configuration (obtained bypassing the preamplifier stage).

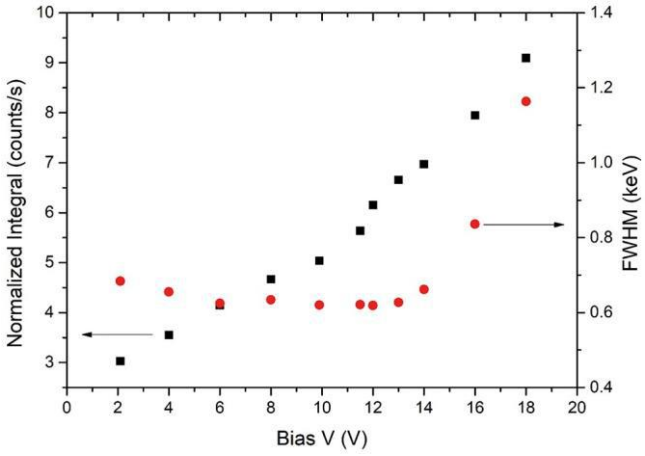

Figure 4. ^{241}Am photopeak integral (black dots, left scale in counts/s) and FWHM (red dots, right scale in keV) of the sample detector as a function of the applied bias voltage.

The spectra of the three sources were then collected at a bias voltage of 12 V, which is a good compromise between high normalised photopeak integral and good resolution (as can be seen in Fig. 4 for the ^{241}Am source). At this bias voltage, the normalised photopeak integral was 6.2 counts s^{-1} for the ^{241}Am peak (E = 59.54keV), 16.3 counts s^{-1} for

the main peak of ^{133}Ba (E = 81keV) and 9.5 counts s^{-1} for the main peak of ^{152}Eu (E =121.78 keV). Fig. 5 shows the spectra of the three sources, which have also been used for determining the energy calibration. The spectra highlight the detector capability to measure the gamma rays emitted by the three sources with energies up to 383.85keV, corresponding to the transition line $\gamma_{3,0}$(Cs) of ^{133}Ba. It is noteworthy that even for the higher energy peaks the energy resolution remains good (1keV at around 350keV). These results together with the low leakage current measured in the diode configuration (Fig. 3) confirm that the method used for the production of the Sb-doped, hole-barrier contact does not compromise the initial high purity of germanium, as already shown by previous experimental measurements of the electrically active defects [24].

Concerning the determination of the detector efficiency, the peculiar geometry of both the detector sample and the experimental setup prevents us from getting a measurement of its absolute efficiency. In fact, it has to be reminded that the gamma-ray sources were put on the side of the detector (see the scheme in Fig. 1) in order to reduce the thickness of the absorbing materials between source and detector. Taking into account the geometrical shape of the detector sample (a 10 × 10 × 2 mm^3 slab), this implies that the solid angle subtended by the detector is not precisely defined. Moreover, the particular geometry of the Sb contact (a central circle with 5 mm diameter) makes it difficult to define the active volume of this detector, since the non-uniform distribution of the electric field, especially close to the detector corners, together with the partial volume depletion give rise to either completely dead or only partly active Ge volume, where the gamma-ray information is lost. This effect is particularly pronounced for the lower-energy gamma rays, which have limited penetration depth (*e.g.* 0.9mm for the 59.54keV line of ^{241}Am and 2mm for the 81keV line of ^{133}Ba). For these reasons, the precise determination of the intrinsic efficiency is postponed to a more suitable detector geometry.

SECTION 2 SEGMENTATION ON NEW N+ CONTACTS

We decided to test the segmentation by using photolithography and etching to open insulating tracks over a continuous junction previously produced on the crystal. In order to test different segmentation parameters we have developed an in-house photolithography process for HPGe. This is a well-known technology for performing the segmentation of contacts in semiconductors but needs some caution when applied to HPGe detectors for avoiding contaminations of the crystal in the processes. In fact, only few companies worldwide sell segmented HPGe detectors.

For most of our developments, we have used small planar HPGe 1 x 1 x 0,2 cm^3 crystals and we will describe the process for segmenting a single-sided planar detector. Before starting the segmentation processes, it is necessary to create both continuous contacts on the planar detector. The segmentation by photolithography can be done only if the contact is very thin (few hundreds of nm). Here we report on the segmentation done on the new antimony (Sb) contact made with the thermal laser annealing process described in section 2. The other contact (p^+ contact) has been done with Boron (B) implantation.

Before starting the photolithography process, the crystal has to be properly cleaned with an appropriated etching. Then we deposit a thin gold layer on the contact to be segmented, which has the purpose of acting as a mask during the last crystal etching at the end of the process. Then, after the thin gold layer has been created, we start the sequence illustrated in Fig. 6.

The photolithography technique is used to segment a HPGe detector. The p-type HPGe detector was etched to remove the cutting damage and to prepare the surface to make contact and junction. A boron contact was performed by ion implantation, while an antimony junction was made by pulse laser melting technique.

On the antimony junction a gold thin layer was deposited, which has the purpose of acting as a mask during the germanium etching.

On the gold layer, we started the photolithography process:

1- We deposited a uniform thin layer of photoresist by using a spin coater;
2- A soft bake at 130°C for 1 minute is necessary to remove solvent on the photoresist layer;

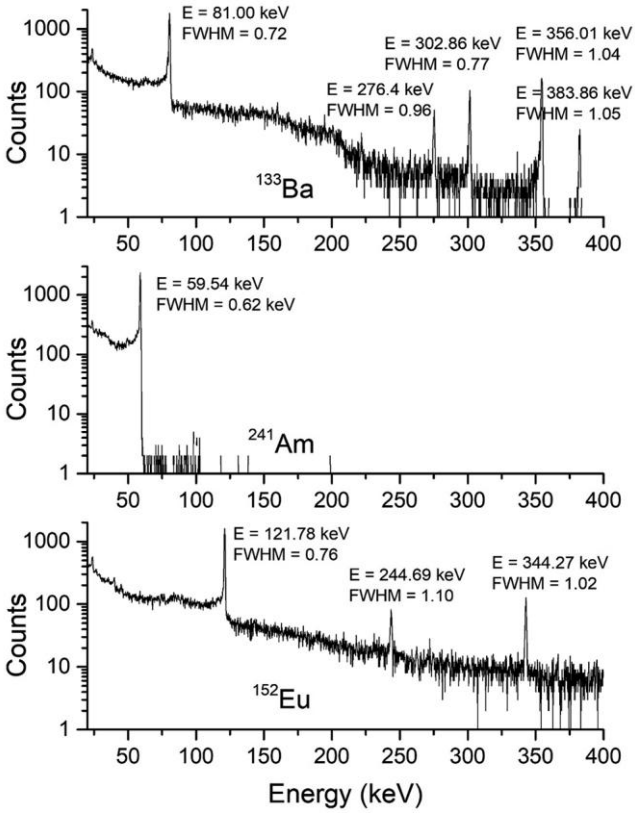

Figure 5. Spectra of ^{241}Am, ^{152}Eu and ^{133}Ba sources collected with a bias voltage of 12V.

3- A photolithographic acetate mask is placed over the surface covered by photoresist and the uncovered photoresist surface is exposed to UV light;
4- The exposed photoresist is removed in a tetramethylammonium bath, and then the detector was rinsed in deionised water to remove completely the dissolved photoresist;
5- A had bake at 130°C for 15 minutes is necessary to hardening the photoresist on the gold layer which guarantees excellent adhesion;
6- A gold etchant bath was performed to remove the gold layer between the segments;
7- The photoresist remained on the gold layer contact is removed with by a hot acetone bath and rinsed in deionised water;
8- The detector is cleaned in an isopropanol bath and the boron contact is protected with kapton tape before performing the germanium etching bath (3 HNO3: 1 HF), thus the etching will be done only on the lateral surface of the detector and between the segments. The etching is necessary to remove the antimony junction outside the contacts. Finally, the etched intrinsic germanium, is passivated with methanol.

As can be noted in Fig. 6 the contacts are well defined as a result of the procedure. In order to avoid possible tip effects when applying voltage, we decided to make rounded edges of both the contacts and the guard ring. The rounded parts of the mask are properly implemented as can be seen by the SEM detail shown in Fig. 7 right. The gap in between segments was 0.4 mm for the first detector.

In order to perform both, the characterisation tests as a diode (I-V plot) and the detector testing through the acquisition of calibration-gamma-source spectra, a new test cryostat has been designed and constructed. This cryostat has an internal variable geometry, vacuum signal feedthroughs and preamplifiers to obtain a pulse with sufficient amplitude for measuring.

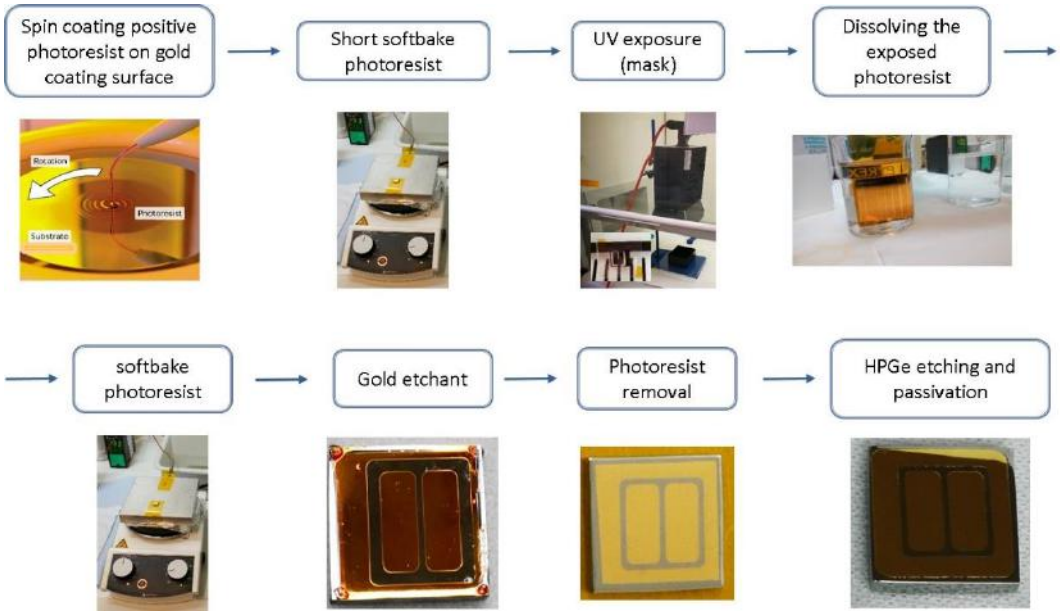

Figure 6. The photolithography process illustrated in our lab.

Figure 7. Photography of the segmented detector (left) and detail of the border of the segment observed by SEM (right).

Both segments exhibit similar behaviour: the counting rate increases with the applied voltage up to nominal value of 18V well inside the I-V plateau. The plateau indicates that we have reached the total depletion voltage Vd at about 15V. The measured resolution is nearly constant (near 0.7keV) for a bias above Vd.

Fig. 9 shows the spectra of ^{241}Am and ^{133}Ba up to 400keV. Higher energies have very low efficiency due to the reduced thickness of the detector (2mm). Both segments of the detector are fully functional and with equivalent performance, indicating that the production of a segmented detector has been successful.

Similar figures are observed for a detector prototype with 0.2mm gap. The reduction of the detector segmentation gap producing a functional detector is as well an achievement in itself, since it will result in detectors with less non-

active surface that might trap part of the collected charges.

The results shown in Fig. 8 and 9 show that it is feasible with the new technology of thermal laser annealing, to obtain a segmented thin n^+-contact on a p-type HPGe crystal suitable for nuclear spectroscopy.

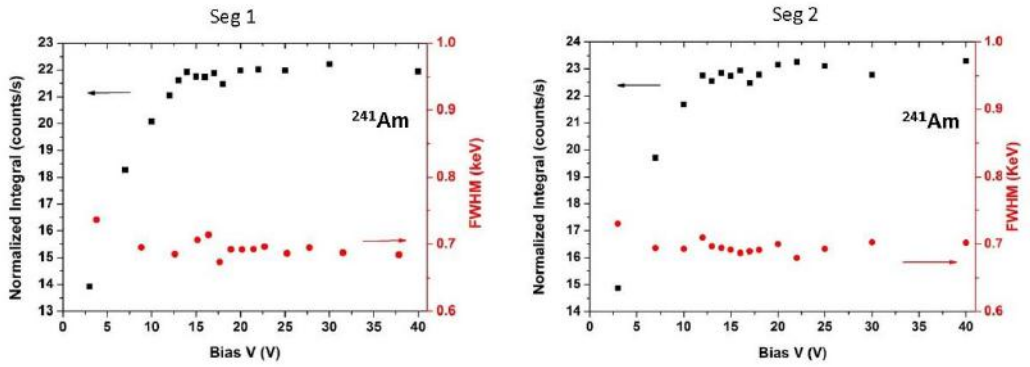

Figure 8. Black squares denote the counting rate (counting rate scale on the left) whereas the red circles show the resolution (FWHM scale on the right), both as function of the applied bias voltage. Both segments show similar behaviour: the counting rate increases with the applied voltage until we reach the depletion voltage.

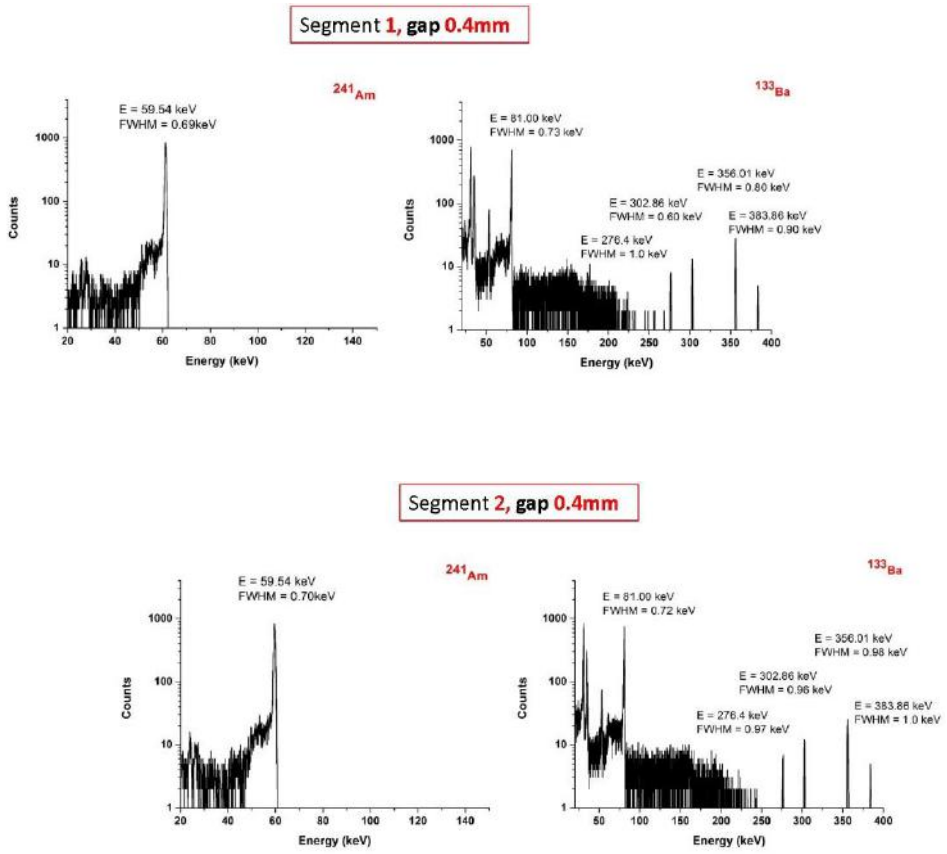

Figure 9. Spectra of ^{241}Am and ^{133}Ba up to 400keV for both segments. Higher energies have very low efficiency because the reduce thickness of the detector (2mm). The gap in between segments is 0.4mm.

CONCLUSION

We have found a new method for the production of a thin hole-barrier contact on high purity germanium, consisting in the deposition of a Sb layer by sputtering, followed by Sb diffusion in HPGe by laser annealing. The method does not jeopardise the high purity of the germanium material and allows to achieve a defect-free surface morphology and a very thin (≤ 100nm) hole-barrier contact. Moreover, the barrier effect is particularly pronounced as highlighted by measurements of the reverse leakage current, which remains very low also in spite of the lack of any guard ring in the rather crude experimental configuration used in the present measurements. It is worth noting that, even if a direct measurement of the electrically active Sb were not yet available, only 1% of the activation would be enough to force the Fermi level of the contact into the conduction band. Accordingly, the hole barrier would become as high as the energy gap. Work is in progress to evaluate the barrier height and the Sb activation. The new method was successfully applied to the realisation of a small detector sample. In spite of the disadvantageous choice of the geometrical configuration of the contacts, which was made privileging the laser treatment at the expense of the detector performance, the sample exhibited very good energy resolution even at the higher gamma-ray energies (300–400keV).

The results of the present work show that the proposed method is particularly promising because:

i) the preparation of Ge surface is not particularly critical for the properties of the hole barrier, therefore its reproducibility is promoted;
ii) a high thermal stability can be foreseen, based on literature data [5, 25];
iii) exploiting the versatility of the described method, further contacts can be developed using different deposition methods (*e.g.,* vacuum evaporation, spin coating [14, 26]), different doping materials (elements of group V for hole-barrier contact and elements of group III for electron-barrier contact) and/or different heating methods (*e.g.* flash annealing [27]).

These preliminary results pave the way to the achievement of a thin, easy to produce and segment, hole-barrier contact in HPGe, which could improve the present performance of position-sensitive, highly segmented HPGe detectors employed by modern gamma-ray tracking spectrometers.